Bio-propylene glycol by liquid phase hydrogenolysis of glycerol with Ni/SiO2-C catalysts

Martín N. Gatti[a,b], Francisco Pompeo[a,b], Gerardo F. Santori[a,b], Nora N. Nichio[a,b,*]

[a] Facultad de Ingeniería, Universidad Nacional de La Plata, 1 esq 47, 1900, La Plata, Argentina
[b] CINDECA, Facultad de Ciencias Exactas, Universidad Nacional de La Plata-CONICET, 47 n° 257, 1900, La Plata, Argentina

ARTICLE INFO

ABSTRACT

The development of catalytic materials, hydrothermally stable and selective to the desired products, is still a challenge. The aim of the present work is to prepare a nickel catalyst with a metal loading of 5 wt% Ni supported on a SiO_2-C composite, to be used in the liquid-phase glycerol hydrogenolysis reaction. The most active and selective catalyst to 1,2-propylene glycol (1,2-PG) was Ni/SC-095, which presented surface acidity fundamentally represented by the presence of carboxylic groups which promoted the C–O cleavage reactions of the glycerol primary carbon to produce acetol, and subsequently by hydrogenation to produce 1,2-PG.

Concerning the selection of operating conditions, the influence of the most relevant variables of the process were analyzed, i.e., temperature (220–260 °C), glycerol concentration (30–65%), and hydrogen partial pressure (0–4 MPa). The best result was obtained at 260 °C with 30 wt% glycerol, 6 h on reaction and a hydrogen partial pressure of 2 MPa. Under these conditions, selectivities of 77% towards 1,2-PG and 3% to acetol were obtained, with 56% of conversion.

It was demonstrated that there are no important structural changes through the characterization of the used samples. Both the SC-095 support and the Ni/SC-095 catalyst maintained their BET surface area. By XRD and TEM, there could be a slight increase in particle size, which would indicate good resistance to sintering against the severe hydrothermal conditions of this reaction.

1. Introduction

Recently, increased attention has been given to the potential of catalytic processes to convert biomass resources into chemical products [1]. Glycerol, a secondary product of biodiesel synthesis which is considered a compound from biomass, can be used in a wide variety of catalytic reactions such as oxidation, hydrogenation, esterification, and reforming, which would allow substituting products that are synthesized by the petrochemical industry [2–4].

In particular, the catalytic hydrogenolysis of glycerol allows obtaining glycols such as 1,3-propylene glycol (1,3-PG), 1,2-propylene glycol (1,2-PG) and ethylene glycol (EG). 1,2-PG and 1,3-PG have a high added value and, depending on their purity, they can be used to manufacture high-resistance polymers, resins, anti-freezing agents, fluids for petroleum extraction, hydraulic fluid, pharmaceutical products, and others [5]. EG is mainly used as an anti-freezing agent. Other major applications of EG include polymers, plastics, electronics, emulsifiers, and surfactants [6,7].

Obtaining 1,2-PG by the catalytic hydrogenolysis of glycerol can be performed in liquid phase, at moderate temperatures (150–300 °C) and pressures between 2 and 8 MPa, avoiding glycerol vaporization and consequently saving energy.

Conventional oxidic supports (e.g., Al_2O_3, SiO_2, ZrO_2, TiO_2) employed in gas-phase reactions are not suitable for aqueous-phase reactions due to hydrolytic attack at elevated temperatures. Most catalytic supports lose their structure under reaction conditions in liquid phase, as in the case of γ-Al_2O_3 which at 200 °C is transformed into boehmite with significant changes in surface area and acidity [8]. This type of behavior has also been observed in phases like δ and θ-Al_2O_3 where the metallic particle suffers a strong sintering due to the presence of water in the reaction medium [9].

Under severe conditions, water may even cause dissociation of Si–O–Si bonds in the SiO_2, which will eventually give rise to another physical structure [10]. For example, the surface area of SBA-15 ordered mesoporous silica decreased from 930 to 31 m^2g^{-1} after a hydrothermal treatment (liquid water at 200 °C for 12 h) due to the pore collapse resulting in the loss of its structural integrity [11,12].

Pham et al. [13,14] developed a method to modify the surfaces of

oxidic supports to make them less susceptible to hydrolytic attack at 200 °C. The approach involves the deposition of a thin film of carbon obtained by controlled pyrolysis of sugars on commercial SiO_2. The results obtained showed a reduced sintering of the metallic particles and almost no leaching. Even though the results are interesting, the difficulty of the method lies in controlling the carbon thickness that is deposited to avoid covering the particle.

Different metal catalysts of Ru [5,15–20], Pt [15–17,20–22] and Pd [15,23,24] have been reported in the literature. Even though the catalysts based on noble metals show adequate levels of activity and selectivity, these precious elements are limited in their application due to their low abundance and high costs. Besides, noble metal catalysts generally present an undesired activity towards the cleavage of C−C bonds.

Xiong et al. [11] reported a deposition–precipitation–carbonization method to prepare highly dispersed Pd/niobia/carbon catalysts with improved hydrothermal stability. They found that the niobia/carbon compounds helped prevent the growth of oxide crystallite size and preserved the Pd dispersion.

Gallegos-Suarez et al. [25] conducted the hydrogenolysis of glycerol (10 wt%, 8 MPa of H_2 and 180 °C) over Ru-based catalysts supported on activated carbon (AC), high surface area graphite (HSAG), multiwalled carbon nanotubes (CNT) and KL-zeolite. They found that in Ruthenium catalysts supported on HSAG and CNT the electron donor character of the respective supports stabilizes electron-rich metal species ($Ru^{\delta-}$) favoring the cleavage of the C−O bond.

Non-noble metal catalysts are mainly based on Cu [15,26–33] and, in particular, Ni [15,28,33,34]. Sepulveda et al. [35] studied the effect of the addition of P_2O_5 (2,3 and 4 wt%) to a Cu/SiO_2 (Cu 20 wt%) catalyst. The increase of catalytic activity in glycerol hydrogenolysis at 220 °C and 5 MPa H_2 was attributed to a combination of electronic and geometric effects induced by the presence of P_2O_5 on the metallic particles of Cu. The Cu-P interaction increased the distance Cu–Cu and, consequently, the electronic density was increased, thus provoking the increase in catalytic activity. This happened with low contents of (2 wt %), while with higher contents of P_2O_5, the formation of aggregates led to the loss of active sites and a consequent decrease in activity.

Dasari et al. [15] evaluated a Ni/C commercial catalyst and obtained a conversion of 40% and a selectivity towards 1,2-PG of 69% at 24 h on stream operating at 200 °C and 1.4 MPa, employing glycerol at 80 wt%. W. Yu et al. [34] employing catalysts of Ni/AC (activated carbon) (Ni 10 wt.%), demonstrated that high nickel dispersions and the acidity generated by the surface oxygenated groups of carbon have a synergic effect on the activity of the hydrogenolysis reaction.

Chau et al. [36] synthesized bifunctional catalysts of Ni and silicotungstic acid (HSiW) supported on Al_2O_3 by a sequential incipient wetness impregnation method (Ni 1 and 10 wt%) for the hydrogenolysis of glycerol (240 °C and 6 MPa H_2). Due to the strong acid character of the catalyst, the main product was 1-propanol. The authors concluded that in order to obtain a desired product selectively, the control of reaction conditions and catalyst properties such as acid strength, the amount of appropriate acid sites, and metal hydrogenation activity will be needed.

Jiménez-Morales et al. [37] prepared and characterized a catalyst of Ni (10 wt% Ni) supported on a support of non-acid SBA-15 mesoporous silica promoted by the addition of cerium (2.5 and 10 wt.% of Ce). The effect of cerium oxide is to act as a strong acid site promoting the formation of acetol, which is later reduced by H_2.

From the above-mentioned studies, it can be concluded that the development of catalytic materials, hydrothermally stable and selective to the desired products, is still a challenge. The aim of the present work is to prepare a nickel catalyst with a metal loading of 5 wt% Ni supported on a SiO_2-C composite, to be used in the liquid-phase glycerol hydrogenolysis reaction. For this purpose, two SiO_2-C composites with different composition were studied to analyze the effect of the support on the activity and selectivity of the catalyst. The nickel catalysts were characterized by different techniques to correlate their activities with the structure of the solids. We also studied the effect of the main operating variables of this reaction, such as temperature, glycerol concentration, reaction time and hydrogen partial pressure.

2. Experimental

2.1. Catalyst synthesis

The gelling property of TEOS (SILBOND 40-AKZO Chemicals) was used in an alcoholic medium (Ethanol 96% from Anedra) to include a phenol-formaldehyde liquid resin (RL 43003, ATANOR, Argentina) in its structure. With subsequent curing and pyrolisis in reducing atmosphere, this resin leaves a high amount of residual carbon.

TEOS and RL 43003, with a 1:1 mass ratio, were mixed on a magnetic stirrer until obtaining an emulsion, to which ethanol was gradually added. Afterwards, pregellification occurred at room temperature for 24 h, drying at 50 °C for another 24 h and complete polymerization by heating to 180 °C (heating rate 10 °C h^{-1}) for 3 h. Finally, calcination took place in a reducing atmosphere during 3 h on an electrical oven at 1580 °C (at 5 °C min^{-1}). This material was denominated SC-095.

A portion of the SC-095 composite was treated with a solution at 10 wt% HF (48 wt% from Aldrich) for 30 min. This solid was washed with distilled water until obtaining a value of neutral pH, filtered and dried at 120 °C for 24 h. The presence of residual H_2F_6Si was eliminated by heating at 400 °C during 1 h. The material thus obtained was denominated SC-015.

The catalysts were prepared by incipient wetness impregnation of Ni ($NiCl_2·6H_2O$ from Sigma-Aldrich) on supports SC-095 and SC-015. Ethanol was used as solvent. The $NiCl_2·6H_2O$ concentration in ethanol was calculated so as to obtain 5 wt% of Ni in the final solid. Then, the solid obtained was dried at 120 °C during 12 h and activated in H_2 (50 cm^3 min^{-1}) at 400 °C for 90 min (10 °C min^{-1}).

2.2. Characterization

The Ni content of samples was determined by atomic absorption spectrometry (Spectrophotometer AA-6650 Shimadzu). The equipment utilized was an IL Model 457 spectrophotometer, with a single channel and double beam.

Adsorption-desorption measurements were performed for a textural characterization. Surface area measurements, the Brunauer–Emmett–Teller (BET) multipoint method and textural analysis were obtained using a Micromeritics ASAP 2020 equipment. The samples were pretreated under vacuum in two 1 h stages at 100 and 300 °C.

XRD patterns were recorded on a Philips 3020 powder diffractometer, using Cu Kα radiation (λ = 1.5418 Å, intensity = 40 mA, and voltage = 35 kV). The patterns were recorded in the range of 2θ = 20°−70°. The crystallite sizes of metallic nickel in the reduced samples were calculated using Scherreŕs equation:

$$d^{XRD} = \frac{K.\lambda}{B.cos(\theta)}$$

Where K was taken as 0.89 and B was the full width of the diffraction line at half of the maximum intensity in radians (Nickel (111) planes).

The acid base properties of supports were determined by the test of isopropanol decomposition (IPA). This reaction was tested in a continuous-flow fixed-bed reactor between 200 and 300 °C, atmospheric pressure, feed 4.5% IPA in Helium, with a flow of 40 cm^3 min^{-1}.

The acidic groups content was determined according to Boehm's method. The titration results allowed obtaining the concentration of carboxylic, lactonic and phenolic groups present in the supports, assuming that $NaHCO_3$ neutralizes carboxylic groups, Na_2CO_3 neutra-

lizes carboxylic and lactonic groups and NaOH neutralizes carboxylic, lactonic and phenolic groups.

To do so, 0.5 g of the sample were added to 30 mL of each one of the following solutions of base 0.025 mol L^{-1}: $NaHCO_3$, Na_2CO_3 and NaOH. The solutions were titrated according to the standardization of this technique [38,39].

Potentiometric titrations were performed with 0.05 g of support suspended in acetonitrile (Merck) and stirred for 3 h. Then, the suspension was titrated with 0.05 mol L^{-1} *n*-butylamine (Carlo Erba) in acetonitrile using a Metrohm 794 Basic Titrino apparatus with a double junction electrode.

Thermogravimetric analyses (DTA-TGA) were performed in a NETZSCH STA 409C/CD instrument. For these assays, 0.02 g of each dried and degassing sample were subjected to a heater from room temperature to 900 °C with a heating rate of 10 °C min^{-1} in a flux of Argon or 90%v/v nitrogen and 10%v/v oxygen composition.

Temperature-programmed reduction tests (TPR) were performed using a conventional dynamic equipment and the response was measured using a TCD and MS detectors. The feed flow was a H_2/N_2 ratio of 1/9 and the heating rate was 10 °C min^{-1} from room temperature up to 1000 °C.

Transmission-electron microscopy (TEM) images were taken by means of a TEM JEOL 100C instrument, operated at 200KV. A graphite pattern was used for calibration. In this analysis, a suspension in 2-propanol was prepared by stirring the solid sample with ultrasound for 10 min. To estimate the average particle size (d_{av}), the particles were considered spherical, and the diameter volume-area was calculated by using expression:

$$d_{av} = \frac{\sum n_i \cdot d_i^3}{\sum n_i \cdot d_i^2}$$

Where n_i is the number of particles with diameter di. Histograms of particle size distribution arose from microphotographs using the technique of clear field image.

2.3. Catalytic activity test

Glycerol hydrogenolysis reactions were carried out in a stainless steel high pressure reactor BR-100 system, from Berghof Instruments, with a volume of 100 mL, operated in batch mode.

The catalyst was reduced ex situ at 400 °C for 90 min in H_2 flow (30 cm^3min^{-1}) using a heating rate of 10 °C min^{-1}. The catalysts were cooled down to room temperature under hydrogen stream and immediately transferred to the reactor containing the glycerol aqueous solution. Then, the reactor was closed, purged and pressurized with pure H_2 (Air Liquide, 99.99%) at 2 MPa. Afterwards, heating was started (6 °C min^{-1}) and when the reactor was at 260 °C, autogenous pressure reached a value of 5,5 MPa and stirring began. The magnetic stirring was set at 1000 rpm to ensure kinetically controlled conditions.

After reaction, the system was cooled to ambient temperature and liquid and gaseous samples were collected. For the analysis and quantification of gaseous products, a Shimadzu GC-8A chromatograph equipped with a thermal conductivity detector (TCD) with a Hayesep D 100–120 column was used. For the analysis and quantification of liquid products a GCMS-QP505A Shimadzu chromatograph was used,equipped with a 19091S-001 HP PONA, 50 m capillary column and with FID and MS detectors.

The accuracy of the measured values was within 5%, and the experiments could be reproduced with a relative error of 10%. Carbon balance for all runs was close to within 98%.

The total conversion of glycerol (X_G) was determined as follows:

$$X_G \ (\%) = \frac{\text{moles of consumed glycerol}}{\text{moles of initial glycerol}}.100\%$$

The selectivity and yield to liquid products were defined as:

Table 1
Textural properties of SC-095 and SC-015.

Sample	Si/C mass ratio	S_{BET} [a]	V_p [b]	Micropores		Mesopores	
				S_{micro} [c]	V_{micro} [c]	S_{meso} [d]	V_{meso} [d]
SC-095	0.95	208	0.48	55	0.02	153	0.46
SC-015	0.15	678	1.42	257	0.11	421	1.31
SC-095/260 °C	0.95	209	0.42	45	0.02	164	0.40
SC-015/260 °C	0.14	608	1.14	255	0.09	353	1.05

[a] Specific surface area ($m^2 g^{-1}$).
[b] Total pore volume ($cm^3 g^{-1}$).
[c] Specific surface area ($m^2 g^{-1}$) and total pore volume for micropores ($cm^3 g^{-1}$).
[d] Specific surface area ($m^2 g^{-1}$) and total pore volume for mesopores ($cm^3 g^{-1}$).

$$S_i \ (\%) = \frac{\text{moles of carbon in specific product}}{\text{moles of consumed glycerol. } 3}.100\%$$

$$Yield_i \ (\%) = \frac{\text{moles of carbon in specific product}}{\text{moles of initial glycerol. } 3}.100\%$$

3. Results and discussion

3.1. Support characterization

The SiO_2-C composites employed as catalytic support were characterized employing various techniques. The Si content was determined from the weight loss produced by oxidation and followed by thermogravimetry (TPO/TGA). In this way, the SC-095 support had a mass ratio of Si/C = 0.95. As indicated in the Experimental section, the support denominated SC-015 was obtained from the SC-095 support treated with HF. Due to this treatment, the content of Si decreases and the mass ratio Si/C is 0.15.

Both supports present type IV N_2 adsorption-desorption isotherms with H3 hysterisis loops, characteristic of mesoporous materials. Table 1 shows the results of BET specific surface area and total pore volume. The SC-095 support present the smallest specific surface, approximately 200 $m^2 g^{-1}$, while the SC-015 support presents a specific surface of 678 $m^2.g^{-1}$ and a greater contribution of the micropores which could have been generated by the HF treatment. A similar effect has been observed during acid treatments in the functionalization of activated carbons with HNO_3 [40].

In order to evaluate the hydrothermal stability of the support, the support composites were characterized after being treated in hot water (260 °C) and reducing atmosphere (5 MPa H_2) for 24 h. These samples were denoted as SC-095/260 °C and SC-015/260 °C. No changes were observed in the Si content by TPO/TGA, so that Si leaching can be discarded. According to Table 1, the SC-095 support is the most stable [41].

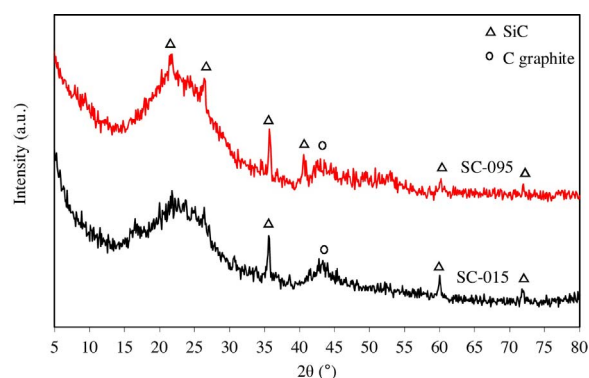Fig. 1 shows that the X-ray diffractograms are quite similar in SC-

Fig. 1. XRD patterns of SC-095 and SC-015.

095 and SC-015. The presence of a band between 2θ = 15 and 30° is observed, characteristic of the silica amorphous band [42,43]. A signal at 2θ = 43.7° assigned to the (1 0 0) plane of the hexagonal phase of graphitic carbon (○) [43,44] can be observed as well as the peaks at 2θ = 21.8°, 26.4°, 35.7°, 41.4°, 60.0° and 71.9° assigned to the (0 0 4 8), (0 1 1), (1 1 1), (2 0 0), (2 2 0) and (3 1 1) planes of silicon carbide (Δ) (JCPDS 29–118, JCPDS 29–129) [45,46]. The peaks corresponding to the graphitic carbon hexagonal phase (1 0 2), (0 0 4) and (1 0 3) at 2θ = 51°, 54.5°, 59° respectively cannot be distinguished. This could be due to the formation of turbostratic carbon. In the literature, it has been reported that turbostractic carbon is a graphitic carbon whose structural planes are rotated and translated with respect to their normal conformation. The presence of turbostractic carbon provokes a shift of the peaks to lower angular values of 2θ and, in this case, they could overlap the silica amorphous band [47].

The surface acid-base properties of the support are very important in the glycerol hydrogenolysis reaction due to the fact that the acid sites promote the dehydration of glycerol. To evaluate these properties, various techniques were used which complement each other: potentiontiometric titration, isopropanol decomposition reaction and the Boehm titration technique.

By means of potentiometric titration with *n*-butylamine, it is possible to estimate the strength and number of the acid sites present in the solid. It is considered that the initial potential (E_i) indicates the maximum strength of the acid sites, while the value of mmol of *n*-butylamine per gram of sample consumed until reaching a plateau in the titration curve (Fig. 2) indicates the total number of acid sites present in the titrated sample [48,49].

The acidic strength of surface sites can be assigned according to the following ranges: very strong site, $E_i > 100$ mV; strong site, $0 < E_i < 100$ mV; weak site, $-100 < E_i < 0$ mV and very weak site, $E_i < -100$ mV. Table 2 shows that total acidity is greater for the SC-015 support, and the acid sites are weak.

The isopropanol decomposition reaction (IPA) was also employed to characterize these supports. This reaction has been reported as an indirect measure to characterize acidity, basicity and strength of sites. They are classified according to their capacity to dehydrate or dehydrogenate, leading to the formation of propylene, diisopropyl ether (DIPE) and water by dehydration, or the formation of acetone and hydrogen by dehydrogenation. When propylene and DIPE are produced, surface sites are strong Lewis acid and base sites. When propylene and acetone are produced, weak Lewis acid sites or strong base sites can be found. If the only reaction product is propylene, the sites can be either strong Lewis or Brønsted acids [50].

The results of this reaction using SC-095 and SC-015 in the 200–300 °C temperature range indicate that the activity was much higher for the SC-015 support, which demonstrates the greater number
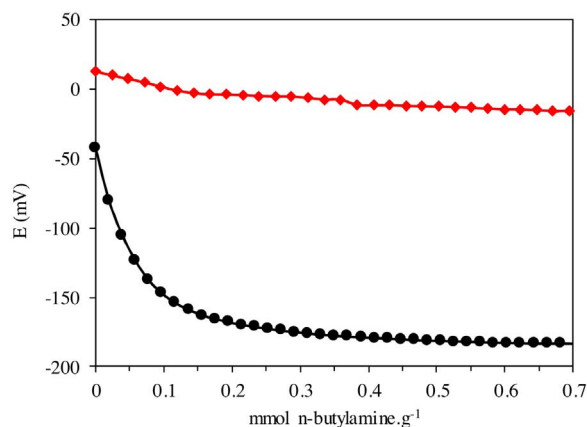
Table 2
Acidic strength and number of acid sites of SC-095 and SC-015 by means of potentiometric titration.

Sample	E_i (mV)	Acidic strength	N° acid sites (mmol *n*-butylamine g^{-1})
SC-095	12.6	Strong	0.18
SC-015	−42.7	Weak	0.40

Table 3
Conversion (X_{IPA}) and selectivities towards propylene ($S_{propylene}$), acetone ($S_{acetone}$) and di-isopropylether (S_{DIPE}) in isopropanol decomposition reaction.

Sample	T (°C)	Conversion X_{IPA}%	Selectivity (%)		
			$S_{propylene}$	$S_{acetone}$	S_{DIPE}
SC-095	260	6	51	47	2
SC-015	260	24	96	3	1
SC-015	220	6	86	9	5

Reaction conditions: 4.5% IPA in Helium 40 cm^3 min^{-1}.

of surface active sites. Table 3 shows the results of selectivity towards propylene, acetone and diisopropyl ether (DIPE) for the same level of conversion (6%). For the SC-095 sample, the selectivity towards propylene and acetone is similar which indicates the presence of weak Lewis acid sites. The higher selectivity towards propylene of SC-015 would indicate a greater contribution of strong Lewis acid sites or Brønsted acid sites.

The presence of DIPE in very low amounts indicates a low concentration of strong Lewis acid sites.

The Boehm titration technique applicable to carbon-based materials allows the identification and quantification of surface acid oxygenated groups [38,39]. The technique is based on the treatment with different alkaline solutions in order to neutralize their surface oxygenated groups. This technique assumes that carboxylic groups are neutralized with a weak base like $NaHCO_3$, while stronger bases like Na_2CO_3 neutralize carboxylic and lactonic groups.

When NaOH is employed, carboxylic, lactonic and phenolic groups are neutralized. If HCl is employed instead of NaOH, by an analogous procedure, it is possible to estimate the total concentration of basic sites of the material, even though the differentiation of basic oxygenated groups has not been reported in the literature [51,52].

Table 4 shows the results of the Boehm titration. It can be observed that the total acidity of the SC-015 support is higher, in agreement with the results of both the potentiometric titration and the decomposition reaction of IPA. As regards the surface groups, the presence of carboxylic groups is slightly higher for SC-095 while the presence of lactonic and phenolic groups is greater for SC-015.

Concerning basicity, SC-095 has a greater content of basic sites which could be groups of pyrones and quinones [51,53], coinciding with the higher selectivity to acetone obtained in the dehydrogenation reaction of IPA.

Fig. 2. Potentiometric titration curves with *n*-butylamine in acetonitrile of SC-095 (♦) and SC-015 (●).

Table 4
Surface oxygenated groups of SC-095 and SC-015, according to standardization of the Bohem titration.

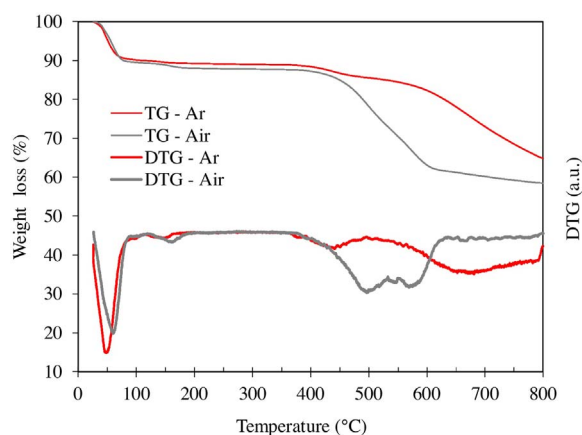| Sample	Acidic surface groups (mmol g^{-1})			Total acidity (mmol g^{-1})	Total basicity (mmol g^{-1})
	Carboxyl group −COOH	Lactonic group −CO−C=O	Phenol group −COH		
SC-095	0.220	0.004	0.034	0.259	0.058
SC-015	0.177	0.019	0.106	0.302	0.018

Fig. 3. Thermogravimetric analysis for Ni/SC-095.

3.2. Catalyst characterization

After the support impregnation with nickel chloride, the samples were calcined in Argon atmosphere. Fig. 3 shows the decomposition profiles of the metallic precursor by thermogravimetry (TGA) for the Ni/SC-095 sample. Three well-differentiated peaks were observed. The weight loss at temperatures below 150 °C is 9 wt% and is assigned to water loss. The second peak, at 440 °C, corresponds to a loss of 5 wt% and is assigned to decomposition of $NiCl_2$ [54]. The third peak, at 650 °C, corresponds to 25 wt% and is assigned to the gasification of the support.

Besides, it can be observed that for heating in air flow, in the 400–620 °C temperature range, both the $NiCl_2$ decomposition and the support gasification occur simultaneously.

Concerning the metallic content of catalysts, it was determined by AAS that the Ni content is very close to the nominal 5% value: 4.5 wt% for Ni/SC-095 and 4.7 wt% for Ni/SC-015.

Fig. 4 shows the TPR profiles for catalysts Ni/SC-095 and Ni/SC-015 are very similar. There is a reduction event at 360 °C with a shoulder at 400 °C, which would correspond to nickel species with middle interaction with the support. At 560 °C, the signal corresponds to H_2 consumption which is accompanied by the release of CO, CO_2 and CH_4, for this reason this event is assigned to the gasification of the support.

Fig. 5 shows the X-ray diffractograms for the catalysts activated in H_2 at 400 °C. It is possible to observe the presence of peaks at $2\theta = 44.4°$, 51.7° and 76.3°, corresponding to planes (1 1 1), (2 0 0) and (2 2 0) of the cubic phase of metallic nickel (▲) (JCPDS 04-0850). No NiO peaks are observed. The crystal sizes calculated by Scherrer's equation are 12.2 nm for Ni/SC-095 and 8.6 nm for Ni/SC-015.
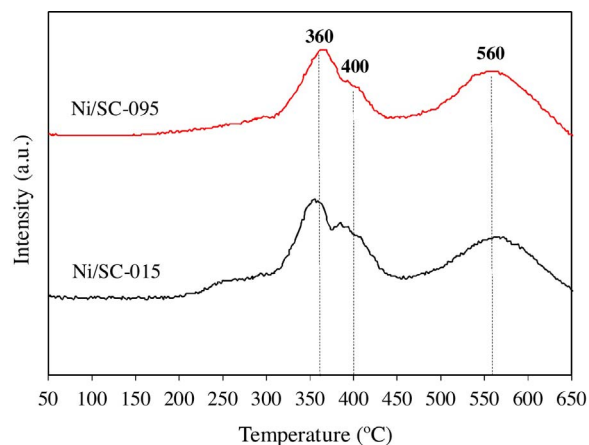

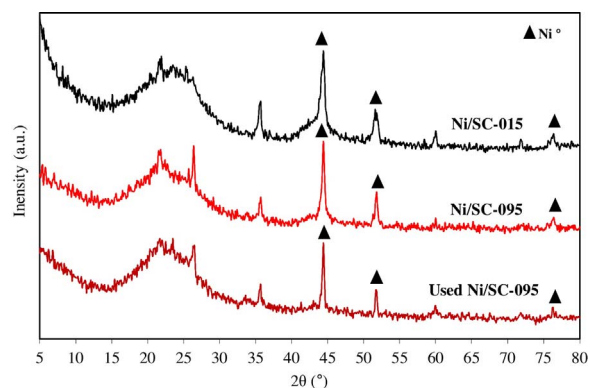**Fig. 4.** TPR profiles of Ni/SC-095 and Ni/SC-015.

Fig. 5. XRD patterns of Ni/SC-015, Ni/SC-095 reduced fresh catalysts and used Ni/SC-095 catalyst.

By TEM it was determined that the distribution of metallic particle size is between 4 and 15 nm with an average diameter d_{av} of 8.5 nm for Ni/SC-095 and 8.4 nm for Ni/SC-015 (Fig. 6 (a) and (b), respectively) which would correspond to metallic dispersions in the order of 11%. The particle size distribution histograms show a greater contribution of 4 nm particles in the NiSC-095 sample. However, this has little incidence on the calculation of the average particle size (d_{av}).

3.3. Catalytic activity

A reaction mechanism has been proposed for glycerol hydrogenolysis based on a first dehydration stage of C−O bond cleavage reactions to produce acetol (AcOH) or 3-hydroxypropanaldehyde as intermediate products and a subsequent hydrogenation stage to produce 1,2-PG or 1,3-PG [16].

On the other hand, the C−O bond cleavage reactions can convert 1,2-PG or 1,3-PG to 1-propanol (1-POH) or 2-propanol (2-POH). Methanol, ethylene glycol and ethanol can be side products due to the occurrence of the C−C bond cleavage reactions.

The results of the catalytic activity in the liquid-phase glycerol hydrogenolysis reaction are shown in Table 5. It can be noticed that even though catalysts Ni/SC-095 and Ni/SC-015 were active, catalyst Ni/SC-095 reaches higher glycerol conversions.

The obtention of gaseous products was very low, less than 4% conversion (mainly CO_2 and CH_4). The reaction products in liquid phase identified and quantified were C1: methanol (MeOH), of C2: ethanol (EtOH), ethylene glycol (EG), of C3: acetone (AcO), 1-propanol (1-POH), acetol (AcOH), 1,2 propylene glycol (1,2-PG) and 1,3 propylene glycol (1,3-PG). Table 5 shows the product distribution and it can be noticed that the selectivity towards C1 and C2 is low if compared with results obtained with noble metal catalysts like Ru [5,18,19] and Pt [20–22] that have a high capacity of C−C bond cleavage.

Besides, it can be observed that catalysts Ni/SC-095 and Ni/SC-015 present high selectivity towards C3 but low selectivity towards AcOH, if compared with results obtained with Cu catalysts, which demonstrates the higher hydrogenating activity of Ni [27,29,30].

In Table 5 it can also be observed that the higher yield of 1,2 PG is obtained with the Ni/SC-095 catalyst. The results with a similar conversion level (15–17%) allow comparing the differences in the product distribution of C3. The most significant difference is that the Ni/SC-015 catalyst presents a higher selectivity towards 1-POH and 1,3-PG. This would be indicating a greater capacity of the C−O bond cleavage which allows obtaining 1-POH from 1,2-PG and 1,3-PG.

In previous studies, we have determined that the metallic dispersion affects the C−C and C−O bond cleavage reactions. However, the C−O bond cleavage reactions are favored when the metallic dispersion decreases from 60 to 20% [55]. The small differences in particle size observed by TEM would not allow explaining the differences in
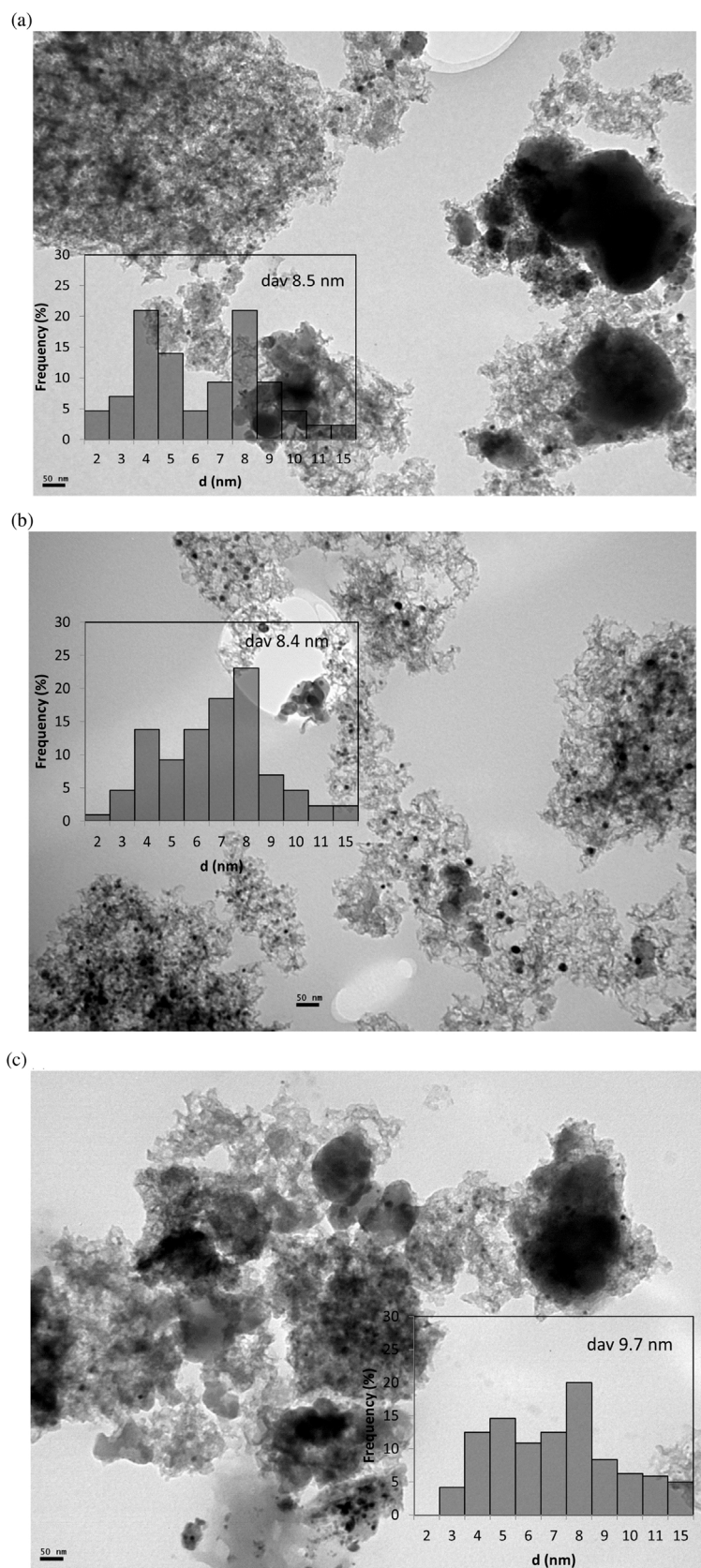
(a)

(b)

(c)

Fig. 6. TEM micrographs of reduced fresh catalysts and particle size distribution: (a) Ni/SC-095 (b) Ni/SC-015 (c) used Ni/SC-095 catalyst.

Table 5
Catalytic performance of Ni/SC-095 and Ni/SC-015 in the liquid phase hydrogenolysis of glycerol.

Catalyst	Time (h)	$X_{G (\%)}$	Selectivity (%)								Yield (%)
			C1	C2	C3	AcO	1-POH	AcOH	1,2-PG	1,3-PG	1,2-PG
Ni/SC-095	0.5	8	2.7	14.3	83.0	1.3	6.6	4.6	70.5	0.0	5.6
	1.0	15	2.7	14.4	82.9	0.6	6.0	4.3	72.0	0.0	10.8
	2.0	30	2.9	13.1	84.0	0.4	2.7	6.9	74.0	0.0	22.2
	4.0	45	1.8	12.0	86.2	0.6	5.9	3.2	76.5	0.0	34.4
	6.0	56	1.8	7.0	91.2	0.6	10.0	3.3	77.3	0.0	43.3
Ni/SC-015	0.5	3	2.1	6.0	90.9	2.8	18.5	8.5	49.5	11.6	1.5
	1.0	5.5	1.8	9.2	89.0	4.0	20.0	8.0	47.0	10.0	2.6
	2.0	10	2.1	6.2	91.7	6.9	28.2	7.8	39.0	9.8	3.9
	4.0	17	2.7	9.3	88.0	7.0	40.5	6.1	30.0	4.4	5.1
	6.0	24	2.8	9.1	88.1	2.8	46.5	5.6	28.8	4.4	6.9

Reaction conditions: 260 °C, P_{H2} initial = 2 MPa, 30 wt% glycerol aqueous solution, catalyst/glycerol = 0.16 (mass ratio).
[a] X_G glycerol conversion.
[b] AcO: acetone, 1-POH: 1-propanol, AcOH: acetol, 1,2-PG: 1,2-propylene glycol, 1,3-PG: 1,3-propylene glycol.
[c] C1: methanol, C2: ethanol + ethylene glycol, C3: AcO + 1-POH + AcOH + 1,2-PG + 1,3-PG.

selectivity.

The presence of 1,3-PG could be explained by the formation of 3-hydroxypropanaldehyde, intermediate compound coming from the secondary carbon dehydration of glycerol, as reported in the literature [18,56]. According to the results obtained by Zhu et al. and references therein cited, it is clearly stated in the literature that Brønsted acid sites favor the removal of the secondary hydroxyl group from glycerol to generate 1,3-PG [57].

The differences between Ni/SC-095 and Ni/SC-015 in activity and selectivity could be attributed to the different acid-base properties of the supports. The presence of functional groups of the lactonic and phenolic type of SC-015, determinated by Boehm titration, could be responsible for favoring the C−O bond cleavage reactions of the secondary carbon of glycerol to produce 1,3 PG and 1-POH [18,56].

Since catalyst Ni/SC-095 presented the best performance, the effect of the main operating variables was studied. Fig. 7 shows the effect of the hydrogen partial pressure on activity.

Studies published in the literature have reported the increase in glycerol conversion with the increase of hydrogen partial pressures for Ru [15,18], Cu [31] and Co [58] catalysts. Sharma et al. [32] worked with Cu-Cr-Zn-Zr catalysts in the range of 1–4 MPa of H_2 and T = 240 °C; they found that glycerol conversion increases with the H_2 partial pressure without affecting the selectivity towards propylene glycol.

Vasiliadou et al. [31], employing a Cu/SiO_2 catalyst between 2 and 8 MPa and 240 °C, reported that the increase in hydrogen concentration positively affects both the rate of reaction and the selectivity towards 1,2-PG.

Our results show that the increase in hydrogen concentration affects conversion very little but it considerably affects the selectivity towards 1,2-PG. Fig. 7 shows that the selectivity towards acetol decreases with hydrogen increase. These results would be indicating that the first stage, the C−O bond cleavage to produce acetol, would not be affected by the presence of H_2.

The effect of temperature in the 220–260 °C range was also studied, which allowed estimating an apparent activation energy $E_{ap} \sim 140$ kJ mol^{-1}, according to an Arrhenius-type law presented in Fig. 8. In the literature were reported values of E_{ap} of 97 kJ mol^{-1} and 132 kJ mol^{-1} were obtained for Cu catalysts, according to Vasiliadou et al. and Sharma et al., respectively [31,32].

The increase in temperature provokes the decrease of the selectivity towards 1,2-PG accompanied by an increase in the selectivity towards C2 (Fig. 9), due to a greater contribution of C−C bond cleavage reactions [15,18,22]. The increase in the selectivity towards AcOH could be due to the fact that hydrogenation is not favored with temperature.

The effect of glycerol concentration was studied, keeping constant the catalyst mass, in the range of 30–65 wt%. Fig. 10 shows that the glycerol conversion decreases as the glycerol concentration increases. This is as expected since the number of active sites is kept constant. The maximum conversion reached is 30% for a glycerol concentration of 30 wt% (at 2 h on reaction). Miyazawa et al. [16] and Balaraju et al.
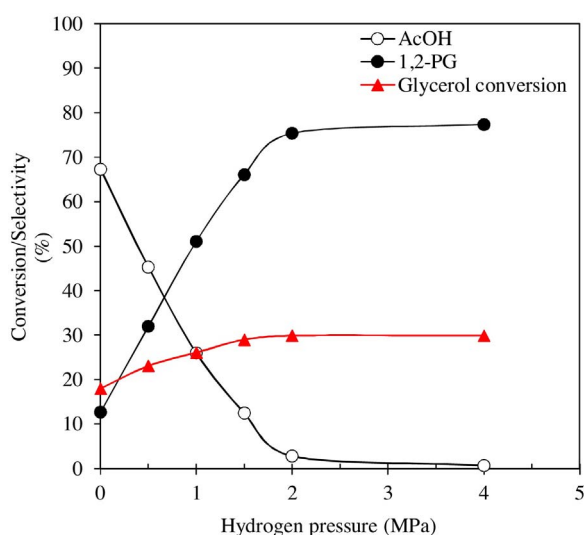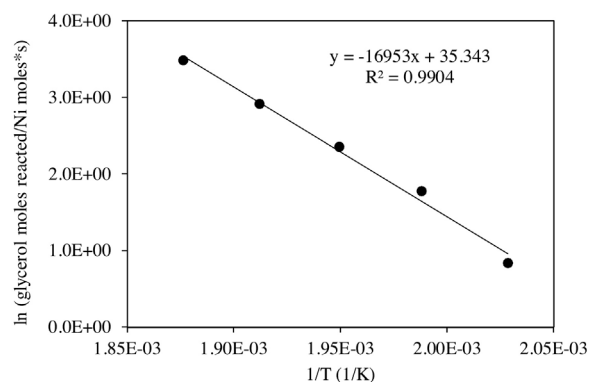

Fig. 7. Glycerol conversion and selectivities to 1,2-PG and AcOH as a function of Hydrogen pressure for Ni/SC-095.Reaction conditions: 260 °C, 30 wt% glycerol aqueous solution, catalyst/glycerol = 0.16 (mass ratio), 2 h.

Fig. 8. Ln (glycerol moles reacted/Ni moles*s) as function of 1/T (1/K) for Ni/SC-095 between 220 and 260 °C.Reaction conditions: P_{H2} initial = 2 MPa, 30 wt% glycerol aqueous solution, catalyst/glycerol = 0.16 (mass ratio), 1 h.
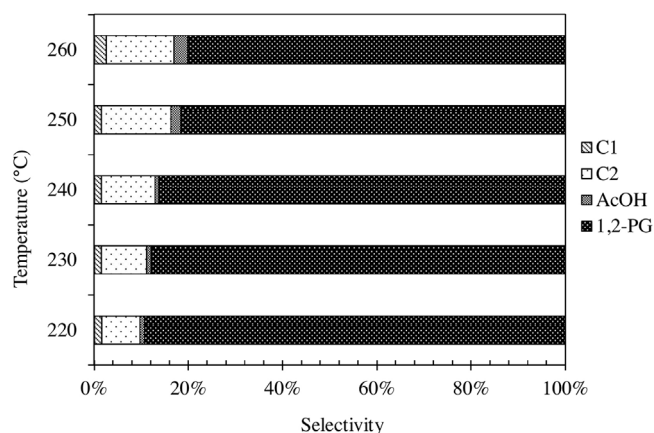
Fig. 9. Effect of reaction temperature over selectivity towards C1 (methanol), C2 (ethanol + ethylene glycol), AcOH and 1,2-PG for Ni/SC-095.Reaction conditions: P_{H2} initial = 2 MPa, 30 wt% glycerol aqueous solution, catalyst/glycerol = 0.16 (mass ratio), 2 h.
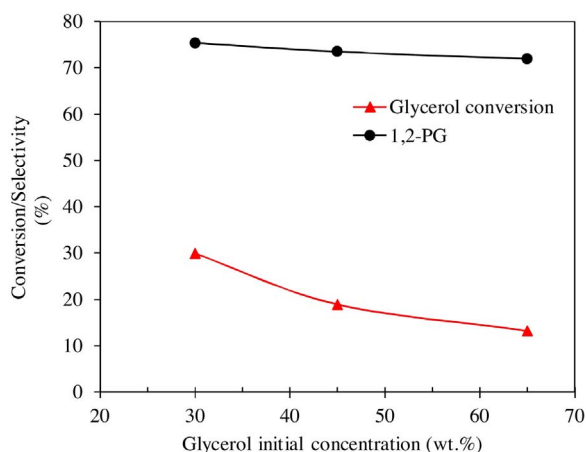

Fig. 10. Effect of initial glycerol concentration over glycerol conversion and selectivity towards 1,2-PG for Ni/SC-095.Reaction conditions: 260 °C, P_{H2} initial = 2 MPa, catalyst/glycerol = 0.16 (mass ratio), 2 h.

[18] reported conversions of 45% for concentrations of glycerol to 10 and 20 wt% respectively.

In Fig. 10 it is observed that the selectivity towards 1,2-PG remains constant with the change in glycerol concentration, suggesting the selective nature of this catalyst.

3.4. Structure changes under reaction conditions

It is important to make sure that the structure of the Ni/SC-095 catalyst is not modified during the catalytic evaluation tests. Thus, the catalyst used in the reaction was washed, dried and then characterized. The S_{BET} of sample Ni/SC-095 used for 6 h is 195 m^2g^{-1}, representing a very small surface reduction in the order of 8%, which is within the experimental error of the technique.

The Ni content in the liquid phase after 6 h on reaction was 100 ppm, determined by the AAS analysis. This would indicate that the Ni loss by leaching is very low, in the order of 4 wt%.

Fig. 5 shows the X-ray diffractogram of the 6 h-used catalyst and of the fresh catalyst. It is not possible to observe the presence of NiO in the used sample. There is a small difference in the width of the Ni^0 peaks, which could be evidencing the presence of bigger crystal sizes.

This is consistent with microscopy results showing an increase in particle size of 8.5 nm in the fresh sample (Fig. 6-a) to 9.7 nm in the 6-h used sample (Fig. 6-c).

The used Ni/SC-095 sample (washed, dried and reduced) was

reused in a 6-h reaction test at 260 °C. A selectivity towards 1,2 PG of 76% was obtained with a glycerol conversion of 49%. If this result is compared with Table 5, it can be observed that conversion decreases by 13%, which is consistent with the increase in particle size. However, further studies will be carried out in order to evaluate the catalytic behavior during several reaction cycles.

4. Conclusions

Ni catalysts were prepared using carbon-based supports which are SiO_2-C composites and are stable against the severe hydrothermal conditions of the liquid-phase glycerol hydrogenolysis reaction. The HF treatment to the SiO_2-C composite generated lactonic and phenolic oxygenated groups on the carbon surface. These groups promoted the formation of 1-POH and 1,3-PG through the C–O bond cleavage reactions of the secondary carbon of glycerol at the expense of 1,2 PG formation.

The most active and selective catalyst towards 1,2-PG was Ni/SC-095, which presented surface acidity fundamentally represented by the presence of carboxylic groups which promoted the C–O bond cleavage reactions of the glycerol primary carbon to produce acetol, and subsequently by hydrogenation to produce 1,2-PG.

Concerning the selection of operating conditions, the influence of the most relevant variables of the process were analyzed, i.e., temperature (220–260 °C), glycerol concentration (30–65%), and H_2 partial pressure (0–4 MPa). The best result was obtained at 260 °C with 30% glycerol, 6 h on reaction and a hydrogen partial pressure of 2 MPa. Under these conditions, selectivities of 77% towards 1,2-PG and 3% to acetol were obtained, with 56% of conversion.

It was demonstrated that there are no important structural changes through the characterization of the used samples. Both the SC-095 support and the Ni/SC-095 catalyst maintained their BET surface area. By XRD and TEM, there could be a slight increase in particle size, which would indicate good resistance to sintering against the severe hydrothermal conditions of this reaction.

Acknowledgments

References

[1] J. Zhang, J. Teo, X. Chen, H. Asakura, T. Tanaka, K. Teramura, N. Yan, ACS Catal. 4 (4) (2014) 1574–1583.
[2] G.W. Huber, S. Iborra, A. Corma, Chem. Rev. 106 (2006) 4044–4098.
[3] D.L. Nelson, M.M. Cox, Lehninger Principles of Biochemistry, fourth ed., W H Freeman & Co., 2004.
[4] J.C. Serrano-Ruiz, R. Luque, A. Sepúlveda-Escribano, Chem. Soc. Rev. 40 (2011) 5266–5281.
[5] S. Bolado, R.E. Treviño, M.T. García-Cubero, G. Gonzalez-Benito, Catal. Commun. 12 (2010) 122–126.
[6] H. Yue, Y. Zhao, X. Ma, J. Gong, Chem. Soc. Rev. 41 (11) (2012) 4218–4244.
[7] O.V. Manaenkov, J.J. Mann, O.V. Kislitza, Y. Losovyj, B.D. Stein, D.G. Morgan, M. Pink, O.L. Lependina, Z.B. Shifrina, V.G. Matveeva, E.M. Sulman, L.M. Bronstein, ACS Appl. Mater. Interfaces 8 (2016) 21285–21293.
[8] R.M. Ravenelle, J.R. Copeland, W. Kim, J.C. Crittenden, C. Sievers, ACS Catal. 1 (2011) 552–561.
[9] K. Lehnert, P. Claus, Catal. Commun. 9 (2008) 2543–2546.
[10] H.L. Castricum, M.C. Mittelmeijer-Hazeleger, A. Sah, J.E. ten Elshof, Microporous Mesoporous Mater. 88 (2006) 63–71.
[11] H. Xiong, H.N. Pham, A.K. Datye, J. Catal. 302 (2013) 93–100.
[12] Y.J. Pagan-Torres, J.M.R. Gallo, D. Wang, H.N. Pham, J.A. Libera, C.L. Marshall, J.W. Elam, A.K. Datye, J.A. Dumesic, ACS Catal. 1 (2011) 1234–1245.
[13] H.N. Pham, A.E. Anderson, R.L. Johnson, K. Schmidt-Rohr, A.K. Datye, Angew. Chem. 124 (2012) 13340–13344.
[14] H.N. Pham, A.E. Anderson, R.L. Johnson, T.J. Schwartz, B.J. O'Neill, P. Duan, K. Schmidt-Rohr, J.A. Dumesic, A.K. Datye, ACS Catal. 5 (2015) 4546–4555.

[15] M.A. Dasari, P.P. Kiatsimkul, W.R. Sutterlin, G.J. Suppes, Appl. Catal. A-Gen. 281 (2005) 225–231.
[16] T. Miyazawa, Y. Kusunoki, K. Kunimori, K. Tomishige, J. Catal. 240 (2006) 213–221.
[17] E.P. Maris, W.C. Ketchie, M. Murayama, R.J. Davis, J. Catal. 251 (2007) 281–294.
[18] M. Balaraju, V. Rekha, P.S. Sai Prasad, B.L.A. Prabhavathi Devi, R.B.N. Prasad, N. Lingaiah, App. Catal. A Gen. 354 (2009) 82–87.
[19] E. Vasiliadou, E. Heracleous, I.A. Vasalos, A.A. Lemonidou, App. Catal. B Environ. 92 (2009) 90–99.
[20] D. Roy, B. Subramaniam, R.V. Chaudhari, Catal. Today 156 (2010) 31–37.
[21] S.N. Delgado, D. Yap, L. Vivier, C. Especel, J. Mol. Catal. A Chem. 367 (2013) 89–98.
[22] S. Zhu, Y. Qiuc, Y. Zhu, S. Hao, H. Zheng, Y. Li, Catal. Today 212 (2013) 120–126.
[23] F. Mauriello, H. Ariga, M.G. Musolino, R. Pietropaolo, S. Takakusagi, K. Asakura, App. Catal. B Environ. 166–167 (2015) 121–131.
[24] Y. Li, H. Liu, L. Ma, D. He, App. Catal. A Gen. 522 (2016) 13–20.
[25] E. Gallegos-Suarez, A. Guerrero-Ruiz, I. Rodriguez-Ramos, A. Arcoya, Chem. Eng. J. 262 (2015) 326–333.
[26] F. Vila, M. López Granados, M. Ojeda, J.L.G. Fierro, R. Mariscal, Catal.Today 187 (2012) 122–128.
[27] Y. Feng, C. Liu, Y. Kang, X. Zhou, L. Liu, J. Deng, H. Xu, Y. Fu, Chem. Eng. J. 168 (2011) 403–412.
[28] M. Akiyama, S. Sato, R. Takahashi, K. Inui, M. Yokota, App. Catal. A Gen. 371 (2009) 60–66.
[29] I. Gandarias, P.L. Arias, J. Requies, M. El Doukkali, M.B. Güemez, J. Catal. 282 (2011) 237–247.
[30] S. Xia, R. Nie, X. Lu, L. Wang, P. Chen, Z. Hou, J. Catal. 296 (2012) 1–11.
[31] E.S. Vasiliadou, A.A. Lemonidou, Chem. Eng. J. 231 (2013) 103–112.
[32] R.V. Sharma, P. Kumar, A.K. Dalai, Appl. Catal. A Gen. 477 (2014) 147–156.
[33] S.M. Pudi, P. Biswas, S. Kumar, B. Sarkar, J. Braz. Chem. Soc. 26 (8) (2015) 1551–1564.
[34] W. Yu, J. Xu, H. Ma, C. Chen, J. Zhao, H. Miao, Q. Song, Catal. Commun. 11 (2010) 493–497.
[35] C. Sepúlveda, L. Delgado, R. García, M. Melendrez, J.L.G. Fierro, I.T. Ghampson, N. Escalona, Catal.Today 279 (2017) 217–223.
[36] T.Q.M. Chau, T.T.F. Ng, Organ. Process Res. Dev. 20 (2016) 1774–1780.
[37] I. Jiménez-Morales, F. Vila, R. Mariscal, A. Jiménez-López, App.Catal. B Environ. 117–118 (2012) 253–259.
[38] S.L. Goertzen, K.D. Thériault, A.M. Oickle, A.C. Tarasuk, H.A. Andreas, Carbon 48 (2010) 1252–1261.
[39] A.M. Oickle, S.L. Goertzen, K.R. Hopper, Y.O. Abdalla, H.A. Andreas, Carbon 48 (2010) 3313–3322.
[40] N. Mager, N. Meyer, A.F. Léonard, N. Job, M. Devillers, S. Hermans, Appl. Catal. B Environ. 148-149 (2014) 424–435.
[41] M.N. Gatti, F. Pompeo, G.F. Santori, N.N. Nichio, XXV Iberoamerican Congress on Catalysis (2016).
[42] H. Ding, J. Li, Y. Gao, D. Zhao, D. Shi, G. Mao, S. Liu, X. Tan, Powder Technol. 284 (2015) 231–236.
[43] T. Niu, G.L. Liu, Y. Liu, Appl. Catal. B Environ. 154–155 (2014) 82–92.
[44] B. Lombardi, F. Pompeo, A.N. Scian, N.N. Nichio, Mat. Lett. 106 (2013) 393–395.
[45] R. Dong, W. Yang, P. Wu, M. Hussain, Z. Xiu, G. Wu, P. Wang, Mat. Charact. 103 (2015) 37–41.
[46] Z. Omidin, A. Ghasemi, S. Bakhshi, Ceram. Int. 41 (2015) 5779–5784.
[47] Z.Q. Li, C.J. Lu, Z.P. Xia, Y. Zhou, Z. Luo, Carbon 45 (2007) 1686–1695.
[48] R. Cid, G. Pecchi, Appl. Catal. 14 (1985) 15–21.
[49] L. Pizzio, M. Blanco, Microporous Mesoporous Mater. 103 (2007) 40–47.
[50] A. Gervasini, J. Fenyvesi, A. Auroux, Catal. Lett. 43 (1997) 219–228.
[51] G.S. Szymánski, Z. Karpinski, S. Biniak, A. Swiatkowski, Carbon 40 (2002) 2627–2639.
[52] H.P. Bohem, Carbon 40 (2002) 145–149.
[53] J. Collins, G. Gourdin, M. Foster, D. Qu, Carbon 92 (2015) 193–244.
[54] C. Popescu, I. Ursu, M. Popescu, R. Alexandrescu, I. Morjan, I.N. Mihailescu, V. Jiano, Thermochim. Acta 164 (1990) 79–90.
[55] M.L. Barbelli, F. Pompeo, G.F. Santori, N.N. Nichio, Catal. Today 213 (2013) 58–64.
[56] E. Gallegos-Suarez, M. Pérez-Cadenas, A. Guerrero-Ruiz, I. Rodriguez-Ramos, A. Arcoya, Appl. Surf. Sci. 287 (2013) 108–116.
[57] S. Zhu, Y. Qiu, Y. Zhu, S. Hao, H. Zheng, Y. Li, Catal. Today 212 (2013) 120–126.
[58] X. Guo, Y. Li, R. Shi, Q. Liu, E. Zhan, W. Shen, Appl. Catal. A Gen. 371 (2009) 108–113.